Journal of Medicinal Chemistry Article

J. Med. Chem. **2010,** *53,* 8619–8626 **8619**
DOI: 10.1021/jm1009742

Synthesis, in Vitro and in Vivo Biological Evaluation, and Comprehensive Understanding of Structure−Activity Relationships of Dipeptidyl Boronic Acid Proteasome Inhibitors Constructed from β-Amino Acids

Yongqiang Zhu,*[,†] Gang Wu,[†] Xinrong Zhu,[†] Yuheng Ma,[†] Xin Zhao,[†] Yuejie Li,[†] Yunxia Yuan,[†] Jie Yang,[†] Sen Yu,[†] Feng Shao,[†] and Meng Lei*[,‡]

[†]*Jiangsu Simcere Pharmaceutical Research Institute and Jiangsu Key Laboratory of Molecular Targeted Antitumor Drug Research, No. 699-18 Xuan Wu Avenue, Xuan Wu District, Nanjing 210042, People's Republic of China, and* [‡]*College of Science, Nanjing Forestry University, No. 159 Longpan Road, Nanjing 210037, People's Republic of China*

Received July 29, 2010

An extensive structure−activity relationship (SAR) study of 72 dipeptidyl boronic acid proteasome inhibitors constructed from β-amino acids is reported. SAR analysis revealed that bicyclic groups at the R^1 position, 3-F substituents at the R^2 position, and bulky aliphatic groups at the R^3 position were favorable to the activities. Enzymatic screening results showed that compound **78**, comprising all of these features, was the most active inhibitor against the 20S human proteasome at less than a 2 nM level, as active as the marketed drug bortezomib. Cellular assays confirmed that compound **78** was the most potent against two hematologic and some solid tumor cells with IC_{50} values less than 1 μM. Pharmacokinetic profiles suggested that **78** showed higher plasma exposure and a longer half-life than bortezomib.

Introduction

The ubiquitin-proteasome pathway (UPP)[a] plays a central role in the protein degradation process and regulates crucial transduction pathways for cell growth and survival, including cell cycle control, transcriptional regulation, cellular stress responses, and antigen presentation.[1,2] Ubiquitin is one of the most conserved proteins in eukaryotes. It is a small 76-amino acid protein that is conjugated to other proteins through an energy-dependent enzymatic pathway,[3] which is facilitated by three different enzymes, E1, E2, and E3. The 26S proteasome, composed of 19S and 20S components, is a multicatalytic complex responsible for degrading most intracellular proteins in eukaryotes. Ubiquitinated proteins are recognized by 19S regulatory units and then translocated into the lumen of 20S proteasome and digested into small peptides therein.[4] Three proteolytic activities are localized to β-subunits present in the 20S proteasome and are classified as chymotrypsin-like (CT-L, β5 subunit), trypsin-like (T-L, β2 subunit), and caspase-like (PGPH, β1 subunit). Of these activities, the CT-L activity was found to be rate-limiting with respect to substrate degradation[5] and has been the focus of drug development.

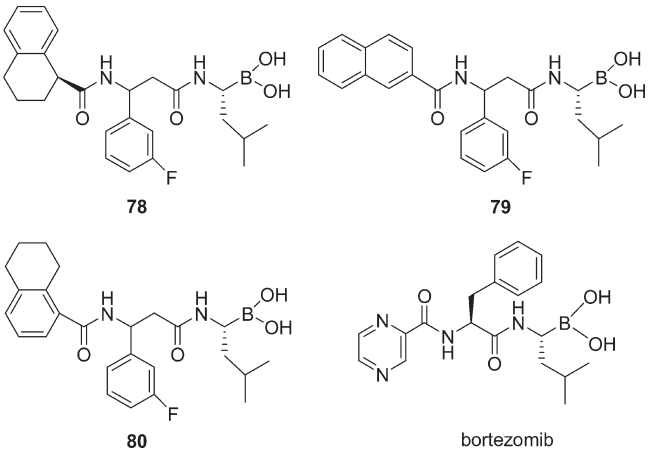

Figure 1. Structures of final compounds and bortezomib.

Clinical validation for the application of proteasome inhibition as a therapeutic strategy was achieved with bortezomib (also named PS-341, structure is shown in Figure 1, Millenium Pharmaceuticals Inc.), a dipeptidyl boronic acid that is intravenously administered and exhibits slowly reversible inhibition of the CT-L activity of the 26S mammalian proteasome.[6−8] On the basis of vital clinical trials, bortezomib has been proven efficacious as a single agent for the treatment of multiple myeloma (MM), non-Hodgkin, and mantle cell lymphoma (MCL).[9−11] Although the toxicity profile of bortezomib is quite well controlled in clinical settings, its side effects include peripheral neuropathy, orthostatic hypotension, pyrexia, cardiac and pulmonary disorders, gastrointestinal adverse events, myelosuppression, thrombocytopenia, asthenia, and pain.[12,13] Consequently, there is a need for the

*To whom correspondence should be addressed. Tel: 86-25-68551686. Fax: 86-25-68551693. E-mail: zhyqscu@hotmail.com. Tel: 86-25-85427621. Fax: 86-25-85427621. E-mail: hk-lm@163.com.

[a] Abbreviations: SAR, structure−activity relationship; UPP, ubiquitin-proteasome pathway; MM, multiple myeloma; MCL, mantle cell lymphoma; MDR, multidrug resistance; CT-L, chymotrypsin-like activity; T-L, trypsin-like activity; PGPH, postglutamyl peptide hydrolysis activity; THNA, tetrahydronaphthalen-1-yl; IC_{50}, inhibition constant; NA, not active; ND, not deteced; DCC, *N*,*N*′- dicyclohexylcarbodiimide; NMM, *N*-methyl morpholine; TMS, tetramethylsilane; HOBt, 1-hydroxybenzotriazole; EDC, 1-ethyl-3-(3-dimethylaminopropyl)-carbodiimide; DIPEA, *N*,*N*-diisopropyl-ethyl-amine; AUC, area under curve; LLOD, lower limit of detection; SRM, selected reaction monitoring; ESI, electrospray source.

Published on Web 11/15/2010

Scheme 1. General Synthesis of N-Terminal-Protected β-Amino Acids **4A1**−**4A48**[a]

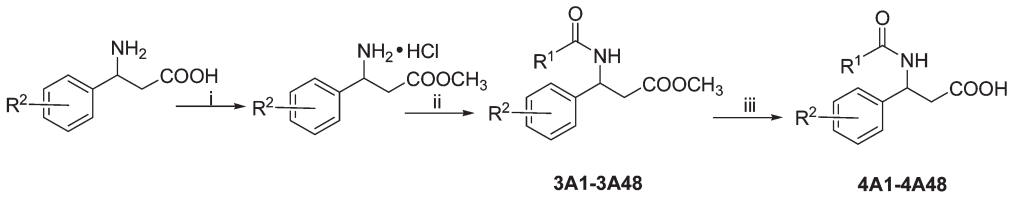

	R^1	R^2		R^1	R^2		R^1	R^2
4A1	Ph	2-F	**4A17**	3-pyridyl	2-F	**4A33**	2-naphthyl	3-Cl
4A2	Ph	3-F	**4A18**	3-pyridyl	3-F	**4A34**	pyrazin-2-yl	3-OMe
4A3	Ph	4-F	**4A19**	3-pyridyl	4-F	**4A35**	2-naphthyl	3-OMe
4A4	Ph	2-Cl	**4A20**	3-pyridyl	2-Cl	**4A36**	1-*(s)*-THNA	3-Cl
4A5	Ph	3-Cl	**4A21**	3-pyridyl	3-Cl	**4A37**	Me	3-OMe
4A6	Ph	4-Cl	**4A22**	3-pyridyl	2-OMe	**4A38**	1-*(s)*-THNA	3-OMe
4A7	Ph	2-OMe	**4A23**	3-pyridyl	3-OMe	**4A39**	1-5,6,7,8-THNA	3-OMe
4A8	Ph	3-OMe	**4A24**	3-pyridyl	2-NO_2	**4A40**	Me	3-F
4A9	Ph	4-OMe	**4A25**	3-pyridyl	3-NO_2	**4A41**	1-*(s)*-THNA	3-F
4A10	Ph	2-NO_2	**4A26**	3-pyridyl	4-NO_2	**4A42**	2-naphthyl	3-F
4A11	Ph	3-NO_2	**4A27**	3-pyridyl	2-Me	**4A43**	1-5,6,7,8-THNA	3-Me
4A12	Ph	4-NO_2	**4A28**	3-pyridyl	3-Me	**4A44**	pyrazin-2-yl	3-F
4A13	Ph	2-Me	**4A29**	1-*(s)*-THNA	3-Cl	**4A45**	Boc	3-Cl
4A14	Ph	3-Me	**4A30**	1-5,6,7,8-THNA	3-Cl	**4A46**	Boc	3-F
4A15	Ph	4-Me	**4A31**	Me	3-Cl	**4A47**	Boc	3-OMe
4A16	Ph	H	**4A32**	pyrazin-2-yl	3-Cl	**4A48**	Cyclohexyl	3-F

[a] Reagents and conditions: (i) CH_3OH, $SOCl_2$, room temperature. (ii) R^1COOH, DCC, HOBt, NMM, THF, 0 °C. (iii) (1) 2 N NaOH, acetone/H_2O, 0 °C; (2) 2 N HCl, H_2O, 0 °C, 44−89.3% yield.

development of proteasome inhibitors with enhanced tolerability and safety profiles.

In an effort to expand the structural diversity of our designed proteasome inhibitors[14,15] and develop novel anticancer drugs, we directed our work to the synthesis of dipeptidyl boronic acid proteasome inhibitors containing unnatural β-amino acid building blocks. The pharmacological activities of a variety of β-amino acids and their derivatives have been well documented.[16−19] β-Amino acids are important components of several natural products. For example, the α-hydroxy-β-phenylalanine component of paclitaxel, a potent anticancer agent, was found to be essential to its antitumor activity,[20] and (*S*)-β-tyrosine was found to be a key component of the antibiotic edeine A.[21,22] In addition, the substitution of α-amino acids for their β-isomers in biologically active peptides renders them resistant to the attack of proteases,[23] which may overcome multidrug resistance (MDR).

In our previous study,[24] several dipeptidyl boronic acid proteasome inhibitors constructed from β-amino acids were synthesized and biologically evaluated in vitro and in vivo. The results showed that this class of compounds was active against 20S human proteasomes and less toxic than bortezomib in vivo. Preliminary structure−activity relationship (SAR) analysis pointed out that three substituents on the peptide backbone greatly influence their biological activities. This warranted further SAR studies including the synthesis of more compounds, from which a lead compound might be identified. In this manuscript, 72 dipeptidyl boronic acid proteasome inhibitors constructed from β-amino acids were synthesized, were biologically investigated, and are discussed in detail with respect to SAR analysis.

Scheme 2. General Synthesis of Amino Boronates Hydrochloride **12**[a]

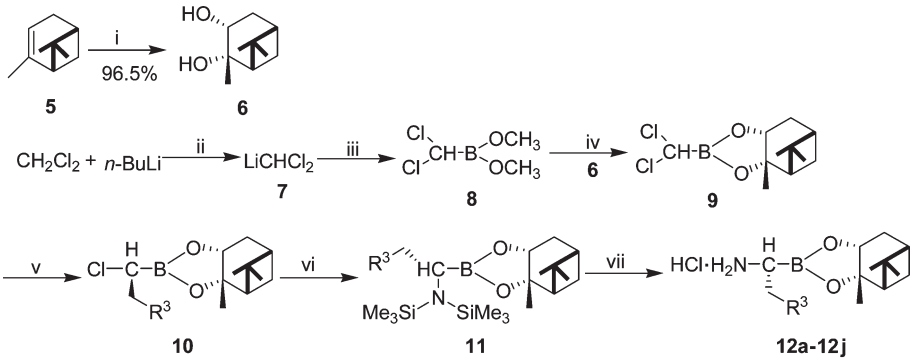

	R^3		R^3
10a, 11a, 12a	$(CH_3)_2CH$	**10f, 11f, 12f**	4-F-Ph
10b, 11b, 12b	$CH_3CH_2CH_2$	**10g, 11g, 12g**	2-Me-Ph
10c, 11c, 12c	Ph	**10h, 11h, 12h**	3-Me-Ph
10d, 11d, 12d	2-F-Ph	**10i, 11i, 12i**	4-Me-Ph
10e, 11e, 12e	3-F-Ph	**10j, 11j, 12j**	Cyclohexyl

[a] Reagents and conditions: (i) OsO_4, *t*-butyl alcohol, trimethylamine *N*-oxide dihydrate, pyridine, water, reflux, 24 h. (ii) THF, −100 °C. (iii) $B(OCH_3)_3$, −100 °C to room temperature. (iv) **6**, THF, room temperature. (v) R^3CH_2MgBr, Et_2O, anhydrous $ZnCl_2$, −78 °C to room temperature. (vi) $LiN(SiMe_3)_2$, THF, −78 °C to room temperature. (vii) Petroleum ether, dry HCl in Et_2O, −78 °C to room temperature.

Scheme 3. General Synthesis of Dipeptidyl Boronic Acids **14**−**85**[a]

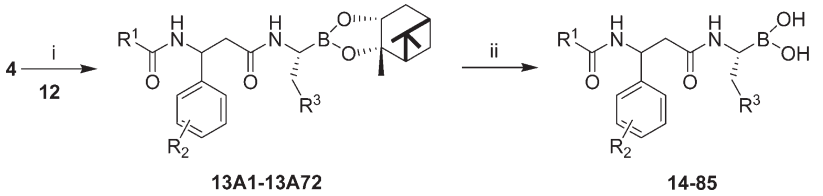

[a] Reagents and conditions: (i) EDC·HCl, HOBt, DIPEA, CH_2Cl_2, −15 °C to room temperature. (ii) Isobutylboronic acid, 2 N HCl, MeOH, hexane.

Results and Discussion

Chemistry. Because of the more difficult synthesis of a chiral *β*-amino acid compared with its racemate, for SAR discussion in this work, racemic *β*-amino acids were employed for fast biological screening. The intermediates of N-terminal protected racemic *β*-amino acids **4A1**−**4A48** were prepared as depicted in Scheme 1. Methyl esters **3A1**−**3A48** were synthesized from various *β*-amino acids, which were obtained from commercial sources using standard peptide synthesis procedures with *N*,*N*′-dicyclohexylcarbodiimide (DCC) and 1-hydroxybenzotriazole (HOBt) as the catalytic coupling agents.[25] After saponification and acidification, various acids **4A1**−**4A48** were gained in moderate to high yields.

The amino boronate hydrochlorides **12** were the key intermediates in the total synthetic route, and following our reported method,[14] hydrochloride salts of structurally diverse amino boronates **12** were prepared from 98% ee (+)-α-pinene (Scheme 2).

Finally, coupling of amino boronates **12** with various acids **4** in the presence of 1-ethyl-3-(3-dimethylaminopropyl)-carbodiimide hydrochloride (EDC·HCl) and HOBt afforded the dipeptidyl boronates **13**, which were used without purification for acid-catalyzed transesterification with isobutylboronic acid to provide target compounds **14**−**85** (Scheme 3).

Biology. Proteasome Inhibition Assay. The capacities of *β*-amino acids-derived dipeptidyl boronic acids to inhibit the CT-L activity of 20S human proteasomes were assayed using appropriate fluorogenic substrates. The marketed bortezomib was used as a standard. Tables 1−3 show the structures and inhibition activities of the novel proteasome inhibitors.

In our previous report,[24] some basic SARs of this class of inhibitors were concluded. The SARs pointed out that substituents with phenyl and *iso*-propyl groups at R^1 and R^3 positions, respectively, were favorable to the activities. Therefore, on the basis of these important findings, initial screening was carried out on the *β*-amino acids at R^2 to elucidate the SAR of this position. For comparison, both phenyl and 3-pyridyl rings were used at the R^1 position.

In our previous study,[24] several para-substituted analogues at the R^2 position were biologically evaluated. The results indicated that the methoxy substituent was the most active. What about the ortho- and meta-substituted analogues? Some electron-withdrawing and electron-donating substituents, such as halogens, nitro, methoxyl, and methyl groups, were introduced at ortho- and meta-positions of the phenyl ring. For comparison of the biological activities in

Table 1. Screening of R^2 Groups of Dipeptidyl Boronic Acid in Inhibiting Human 20S Proteasome CT-L Activity

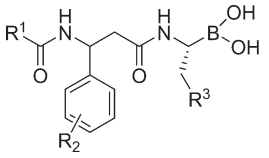

compd	R^1	R^2	R^3	IC_{50} (nM)[a]
14	Ph	2-F	^{i}Pr[b]	38.9
15	Ph	3-F	^{i}Pr	19.0
16	Ph	4-F	^{i}Pr	34.6
17	Ph	2-Cl	^{i}Pr	89.1
18	Ph	3-Cl	^{i}Pr	16.5
19	Ph	4-Cl	^{i}Pr	20.8
20	Ph	2-OMe	^{i}Pr	224
21	Ph	3-OMe	^{i}Pr	46.7
22	Ph	4-OMe	^{i}Pr	32.8
23	Ph	2-NO_2	^{i}Pr	NA[c]
24	Ph	3-NO_2	^{i}Pr	42.6
25	Ph	4-NO_2	^{i}Pr	35.4
26	Ph	2-Me	^{i}Pr	1250
27	Ph	3-Me	^{i}Pr	50.1
28	Ph	4-Me	^{i}Pr	26.3
29	Ph	H	^{i}Pr	39.8
30	3-pyridyl	2-F	^{i}Pr	1100
31	3-pyridyl	3-F	^{i}Pr	NA
32	3-pyridyl	4-F	^{i}Pr	590
33	3-pyridyl	2-Cl	^{i}Pr	NA
34	3-pyridyl	3-Cl	^{i}Pr	22.9
35	3-pyridyl	2-OMe	^{i}Pr	87.0
36	3-pyridyl	3-OMe	^{i}Pr	19.0
37	3-pyridyl	2-NO_2	^{i}Pr	NA
38	3-pyridyl	3-NO_2	^{i}Pr	26.9
39	3-pyridyl	4-NO_2	^{i}Pr	7300
40	3-pyridyl	2-Me	^{i}Pr	1250
41	3-pyridyl	3-Me	^{i}Pr	50.1
bortezomib				1.35[d]

[a] Each IC_{50} determination was performed with five concentrations, and each assay point was determined in duplicate. [b] ^{i}Pr, *iso*-propyl. [c] NA, not active. [d] IC_{50} value obtained for bortezomib under our experimental conditions.

identical conditions, previously reported 4-methyl, 4-methoxy, and 4-chloro substituted analogues were reevaluated. The results are shown in Table 1. Generally, the preference for phenyl ring substitution was meta > para > orhto. For the phenyl substituent at the R^1 position, exploration of R^2 substituents revealed the following activity orders: (1) for meta-substituted phenyl, 3-Cl (**18**, 16.5 nM) > 3-F (**15**, 19.0 nM) > H (**29**, 39.8 nM) > 3-NO_2 (**24**, 42.6 nM) > 3-OMe (**21**, 46.7 nM) > 3-Me (**27**, 50.1 nM); (2) for ortho-substituted phenyl, 2-F (**14**, 38.9 nM) > H (**29**, 39.8 nM) > 2-Cl (**17**, 89.1 nM) > 2-OMe (**20**, 224 nM) > 2-Me (**26**, 1250 nM) > 2-NO_2 (**23**, NA); (3) for para-substituted phenyl, 4-Cl (**19**, 20.8 nM) > 4-Me (**28**, 26.3 nM) > 4-OMe (**22**, 32.8 nM) > 4-F (**16**, 34.6 nM) > 4-NO_2 (**25**, 35.4 nM) > H (**29**, 39.8 nM). For 4-substituted phenyl at the R^2 position, there was no obviously different activity among the various groups, which suggested that the substituents at this position had no crucial interaction with the residues of the active site. However, when the phenyl group was replaced with 3-pyridyl substituent at the R^1 position, the case was quite different: 2-Substituted and 4-substituted phenyl at the R^2 position showed no inhibitory activity or much less potent activity except 2-methoxyl phenyl, while 3-substituted phenyl showed potency in the following order: 3-OMe (**36**, 19.0 nM) > 3-Cl (**34**, 22.9 nM) > 3-NO_2 (**38**, 26.9 nM) > 3-Me (**41**, 50.1 nM) > 3-F (**31**, NA). On the basis of the above information, R^1 and R^2 substituents of compounds **15**, **18**, and **36** (3-F, 3-Cl, and 3-OMe) were incorporated into the next series of compounds with varying R^3 substituents.

Table 2. Screening of R^3 Group of Dipeptidyl Boronic Acid in Inhibiting Human 20S Proteasome CT-L Activity

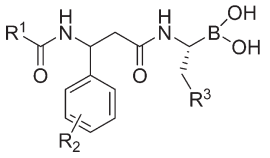

compd	R^1	R^2	R^3	IC_{50} (nM)[a]
42	Ph	3-F	*n*-Pr[b]	1250
43	Ph	3-F	Ph	1200
44	Ph	3-F	2-Me-Ph	NA
45	Ph	3-F	2-F-Ph	301
46	Ph	3-F	3-Me-Ph	120
47	Ph	3-F	3-F-Ph	131
48	Ph	3-F	4-Me-Ph	501
49	Ph	3-F	4-F-Ph	75.8
50	Ph	3-F	cyclohexyl	NA
51	Ph	3-Cl	*n*-Pr	316
52	Ph	3-Cl	Ph	1620
53	Ph	3-Cl	2-Me-Ph	NA
54	Ph	3-Cl	2-F-Ph	371
55	Ph	3-Cl	3-Me-Ph	NA
56	Ph	3-Cl	3-F-Ph	NA
57	Ph	3-Cl	4-Me-Ph	1150
58	Ph	3-Cl	4-F-Ph	194
59	Ph	3-Cl	cyclohexyl	NA
60	3-pyridyl	3-Cl	cyclohexyl	NA
61	3-pyridyl	3-OMe	*n*-Pr	1480
62	3-pyridyl	3-OMe	Ph	1090
63	3-pyridyl	3-OMe	2-Me-Ph	NA
64	3-pyridyl	3-OMe	2-F-Ph	602
65	3-pyridyl	3-OMe	3-Me-Ph	1770
66	3-pyridyl	3-OMe	3-F-Ph	89.1
67	3-pyridyl	3-OMe	4-Me-Ph	930
68	3-pyridyl	3-OMe	4-F-Ph	63
bortezomib				2.57[c]

[a] Each IC_{50} determination was performed with five concentrations, and each assay point was determined in duplicate. [b] *n*-Pr, *n*-propyl. [c] IC_{50} value obtained for bortezomib under our experimental conditions.

Variation of moieties at the R^3 position led to distinct activities and SAR (Table 2). Screened from various substituents, including cyclohexyl, branched and unbranched aliphatic alkyl groups, and aromatic phenyl rings substituted at ortho-, meta-, or para-positions with methyl or fluoro groups, it turned out that compounds substituted by bulky *iso*-propyl at the R^3 position exhibited the most potent activity. For example, compound **36** (19.0 nM, Table 1) containing *iso*-propyl was 78-fold more potent than compound **61** (1480 nM, Table 2) bearing *n*-propyl. *iso*-Propyl substituted compound **18** (Table 1) showed the potent inhibitory effect with an IC_{50} value of 16.5 nM, which was 18-fold more potent than *n*-propyl substituted **51** (316 nM, Table 2). As shown in Table 2, cyclcohexyl substituted compounds **50**, **59**, and **60** showed no activities. Replacement of *iso*-propyl group at the R^3 position of compound **36** (19.0 nM, Table 1) with phenyl (**62**, 1090 nM), 2-methylphenyl (**63**, NA), and 3-methylphenyl (**65**, 1770 nM), respectively, nearly resulted in the loss of activity. The activity obviously

decreased when *n*-propyl (**51**, 316 nM) was replaced with phenyl (**52**, 1620 nM), 2-methylphenyl (**53**, NA), and 3-methylphenyl (**55**, NA). It seems that aromatic and cycloalkyl groups at the R^3 position are not favorable to the activity. However, it is a different case for aromatic groups substituted by fluorine atoms at the R^3 position. Introduction of a fluoro group led to significant improvement of potency. Compound **45** bearing a fluoro group at the ortho-position of the phenyl ring showed a moderate inhibitory effect with an IC_{50} value of 301 nM, and removal of the fluoro group decreased inhibition (**43**, 1200 nM, and **44**, NA). Comparison between other methyl- and fluoro-substituted phenyl rings, such as pairs **48** and **49**, **53** and **54**, **57** and **58**, **63** and **64**, **65** and **66**, and **67** and **68**, also supported this trend. As discussed above, employment of *iso*-propyl at the R^3 position was favorable to the activity, so it was fixed when R^1 substituents were screened.

Optimization of R^2 and R^3 substituents suggested that 3-Cl, 3-F, and 3-OMe at the R^2 position and *iso*-propyl at the R^3 position increased the potency of this class of inhibitors; thus, these groups were maintained at the corresponding positions, while R^1 substituents were optimized. To further study the SAR of dipeptidyl boronic acids constructed from β-amino acids, compounds were synthesized with methyl, bulky Boc and cyclohexyl groups, and aromatic heterocyclic rings at the R^1 position (**69**−**85**). The biological data are listed in Table 3. In general, compounds with bicyclic groups at the R^1 position were more potent than those substituted by monoaromatic heterocyclic and alkyl groups. For 3-pyridyl and pyrazin-2-yl, respectively, substituted **31** (NA) and **81** (269 nM), the IC_{50} values were far lower than those substituted by bicyclic groups, such as **78**, **79**, and **80**. However, replacement of the aromatic groups with methyl (**69**, **74**, and **77**, NA) and Boc groups (**82**, **83**, and **85**, NA) led to a loss of 20S proteasome inhibitory activity. Furthermore, addition of a cyclohexyl group (**84**, 33.1 nM) at the R^1 position resulted in 30-fold loss in potency as compared with compound **78** (1.02 nM). Among them, it is noteworthy to point out that compounds substituted with both 3-F substituents at the R^2 position and bicyclic groups at the R^1 position, such as **78**, **79**, and **80**, were significantly active, with IC_{50} values less than 5 nM, and these compounds were comparable in potency to the marketed bortezomib and therefore selected for further development.

Table 3. Screening of R^1 Group of Dipeptidyl Boronic Acid in Inhibiting Human 20S Proteasome CT-L Activity

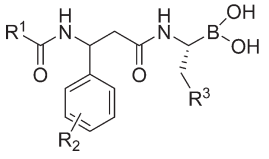

compd	R^1	R^2	R^3	IC_{50} (nM)[a]
69	Me	3-Cl	^{i}Pr[b]	NA
70	pyrazin-2-yl	3-Cl	^{i}Pr	97.7
71	2-naphthyl	3-Cl	^{i}Pr	117
72	1-(*s*)-THNA[c]	3-Cl	^{i}Pr	21.8
73	1-5,6,7,8-THNA	3-Cl	^{i}Pr	190
74	Me	3-OMe	^{i}Pr	NA
75	1-(*s*)-THNA	3-OMe	^{i}Pr	28.1
76	1-5,6,7,8-THNA	3-OMe	^{i}Pr	158
77	Me	3-F	^{i}Pr	NA
78	1-(*s*)-THNA	3-F	^{i}Pr	1.02
79	2-naphthyl	3-F	^{i}Pr	3.01
80	1-5,6,7,8-THNA	3-F	^{i}Pr	3.89
81	pyrazin-2-yl	3-F	^{i}Pr	269
82	Boc	3-Cl	^{i}Pr	NA
83	Boc	3-F	^{i}Pr	NA
84	cyclohexyl	3-F	^{i}Pr	33.1
85	Boc	3-OMe	^{i}Pr	NA
bortezomib				1.54[d]

[a] Each IC_{50} determination was performed with five concentrations, and each assay point was determined in duplicate. [b] ^{i}Pr, *iso*-propyl. [c] THNA, tetrahydronaphthalen-1-yl. [d] IC_{50} value obtained for bortezomib under our experimental conditions.

Cellular Assay Results. For drug development, the three most potent proteasome inhibitors **78**, **79**, and **80** (structures are shown in Figure 1) were further tested in eight human tumor cell lines to determine their effects on cancer cells. The eight cancer cell lines included two hematologic tumors, such as promyelocytic leukemia cell line HL-60, and multimyeloma cell line RPMI 8226, and six solid tumors, comprising human nonsmall cell lung cancer cell line A549, human colon carcinoma cell line SW-480, human ovarian carcinoma SKOV-3, human hepatocellular liver carcinoma cell line HepG2, human prostate cancer cell line PC-3, and human gastric carcinoma cell line BGC-823. The cellular activities of the three compounds and bortezomib are displayed in Table 4. In general, the three compounds showed potent cytotoxicity against most of the cancer cell lines. The two hematologic tumor cell lines were more sensitive to this class of inhibitors than the six solid tumors, which is consistent with the results of dipeptidyl boronic acid proteasome inhibitors composed of α-amino acids.[14] These three inhibitors (**78**, **79**, and **80**) inhibited the two hematologic tumor cell lines at the same level with IC_{50} less than 1 μM, while inhibition of the six solid tumors was comparatively less potent than that of hematologic ones. Across all cell lines, compound **78** was the most potent, which was consistent with results of proteasome inhibition assays. At the same time, it is noteworthy to point out that **78** also effectively interacted with SW-480 and BXPC-3 solid cancer cell lines at less than 1 μM. This compound may therefore possess potential for the treatment of some solid tumors in the future development.

Pharmacokinetics Profiles and Toxicity of 78−80 and Bortezomib. In our previous paper,[24] we discussed the pharmacokinetic profiles of the lead compound **4q**, a dipeptidyl boronic acid constructed from a β-amino acid moiety. It was found that this compound showed a much longer elimination half-life ($T_{1/2}$z) than the marketed bortezomib with iv administration.

Table 4. Cytotoxicity of Compounds against Tumor Cell Lines (IC_{50})[a]

compd	BXPC-3	SW-480	A549	PC-3	SKOV-3	HepG2	HL-60	RPMI 8226
78 (μM)	0.89	0.97	4.36	2.30	2.35	5.24	0.33	0.33
79 (μM)	3.54	2.38	2.02	2.99	8.77	6.99	0.53	0.33
80 (μM)	4.13	3.71	4.16	2.21	12.08	16.57	0.85	0.77
bortezomib (nM)[b]	19.4	12.3	13.9	8.3	66.8	25.2	3.5	3.5

[a] Each cellular IC_{50} determination was performed with 10 concentrations, and each assay point was determined in triplicate. [b] IC_{50} value obtained for bortezomib under our experimental conditions.

Table 5. Single Dose iv and ig Pharmacokinetics Profiles of **78**−**80** and Bortezomib in SD Rats

compd	dose (mg/kg)	T_{max} (h)	C_{max} (ng/mL)	$AUC_{(0-t)}$ (ng h/mL)	$MRT_{(0-t)}$ (h)	$T_{1/2}z$ (h)	Vz (mL/kg)	Clz [(mL/h)/kg]
78[a]	1.0 iv	0.03	2750	1095	1.5	5.5	6757	934
	1.0 ig	ND[b]	ND	ND	ND	ND	ND	ND
79[a]	1.0 iv	0.03	5786	1706	1.4	4.5	3902	576
	1.0 ig	ND[b]	ND	ND	ND	ND	ND	ND
80[a]	1.0 iv	0.03	2650	957	1.4	4.8	6653	1015
	1.0 ig	ND[b]	ND	ND	ND	ND	ND	ND
bortezomib[c]	1.0 iv	0.03	1082	654	1.4	2.0	3744	1433
	1.0 ig	0.23	161	303	7.69	7.47	29791	2683

[a] Diastereoisomers. [b] ND, not detected. [c] All of the data were obtained in our experimental conditions.

Encouraged by these results, we again evaluated the pharmacokinetics profiles of the three drug candidates **78**, **79**, and **80**, which were selected from the results of proteasome inhibition and cytotoxicity assays. The results compared with bortezomib are illustrated in Table 5. After iv bolus injection in male SD rats, all of the three compounds were eliminated slowly with elimination half-lives 2-fold longer than that of bortezomib ($T_{1/2}z$: 5.5, 4.5, and 4.8 vs 2.0 h, respectively). Such long elimination phase half-lives for these compounds are due in part to the larger volume of distribution (Vz = 6757, 3902, and 6653 mL/kg, respectively) and much lower systemic clearance [CLz = 934, 576, and 1015 (mL/h)/kg]. Furthermore, from the area under the curve (AUC) data, it can be concluded that these three candidates had higher plasma exposures in SD rats than the standard bortezomib. However, when intragastrically administered in male SD rats, the concentrations of the three candidates declined below 5 ng/mL after half an hour in plasma, the lower limit of detection (LLOD). This lower oral bioavailability is possibly due to decreased absorption in the mouse gastrointestinal tract and first pass metabolism in the liver. It had demonstrated that the marketed bortezomib showed an approximate 46% oral bioavailability in our test. Although previous studies have shown that bortezomib was orally bioactive,[26,27] current bortezomib therapy in MM and MCL is still intravenous after being marketed for more than 7 years, and no oral formulation was reported.

During the pharmacokinetic evaluation, the in vivo toxicity of these three candidates and bortezomib was also observed. At 1.0 mg/kg iv and ig doses of bortezomib, all of the SD rats died after 10 h, while the SD rats in the group of three compounds did not show any toxic reactions, which was consistent with our previous ovservation.[24]

Conclusion

In this manuscript, an extensive understanding of SAR of a series of novel dipeptidyl boronic acid proteasome inhibitors constructed by β-amino acids was disclosed. By varying different substituents at R^1, R^2, and R^3 positions of the backbone, 72 novel compounds were synthesized and biologically evaluated against the 20S human proteasome. On the basis of the proteasome assay results, some SARs of R^1, R^2, and R^3 substituents were summarized. From the screening results, compound **78** showed the most potent activity with IC_{50} values of less than 2 nM and 1 μM in proteasome inhibition and hematologic tumor cell line cytotoxicity evaluations, respectively. Compound **78** was also much more active against some solid tumor cell lines and has been selected as a development candidate. Pharmacokinetic profiles suggested candidate **78** showed a higher plasma exposure and longer half-life than bortezomib and is also less toxic than the control. Current studies provide a good starting point to develop novel dipeptidyl boronic acid proteasome inhibitors derived from β-amino acids.

Experimental Section

Chemistry. Commercially available reagents were used directly without any purification unless otherwise stated. Absolutely anhydrous solvents were obtained with the proper methods introduced in the literature. Yields refer to chromatography unless otherwise stated. Reactions were monitored by thin-layer chromatography carried out on silica gel aluminum sheets (60F-254) and RP-18 F254s using UV light as a visualizing agent, 15% ethanolic phosphomolybdic acid and heat, or ninhydrin and heat as a developing agent. Column chromatography was performed on 200−300 mesh silica gel and an ODS C-18 column. Analytical reverse phase high-performance liquid chromatography (HPLC) was run using a Kromasil 100-5C18, 4.6 mm × 250 mm column eluting with a mixture of methanol and water containing 0.02% triethylamine and 0.03% trifluoacetic acid. HPLC showed that purity of all of the final products was greater than 95%. Melting points were obtained on an YRT-3 melting point apparatus and were uncorrected. ^{1}H NMR and ^{13}C NMR spectra were recorded at room temperature on BRUKER Avance 300 or Avance 500 spectrometers. Chemical shifts are reported in ppm (δ units), and tetramethylsilane (TMS) was used as an internal reference. Coupling constants (J) are expressed in hertz. Mass spectra were obtained using Agilent LC-MS (1956B) instruments in electrospray positive and negative ionization modes. High-resolution mass spectra were recorded on a ZAB-HS instrument using an electrospray source (ESI).

The synthesis of significantly active compounds **78**−**80** is indicated below. Detailed synthesis and spectral data of intermediates **4A1**−**4A48**, **6**, **9**, **10a**−**j**, **12a**−**12j**, and the target compounds **14**−**77** and **81**−**85** are described in the Supporting Information.

(*R*)-1-[3-(3-Fluorophenyl)-3-((*S*)-1,2,3,4-tetrahydronaphthalene-4-carboxamido)propanamido]-3-methylbutyl Boronic Acid (78). To a cooled solution (−5 °C) of 3-(3-fluorophenyl)-3-((*S*)-1,2,3,4-tetrahydronaphthalene-4-carboxamido)propanoic acid **4A41** (0.34 g, 1.00 mmol) dissolved in anhydrous CH_2Cl_2 (30 mL) was added HOBt (0.16 g, 1.20 mmol). After 20 min, the temperature of the reaction system was cooled to −15 °C, and EDC·HCl (0.19 g, 1.00 mmol) was added. Finally, the precooled (0 °C) mixture of the known pinanediol boronate amino hydrochloride **12b** (0.30 g, 1.00 mmol) and DIPEA (0.26 mL, 1.48 mmol) in anhydrous CH_2Cl_2 (10 mL) was poured. The mixture was stirred at −15 °C for 1 h and at room temperature for 2 h and finally quenched with water. The aqueous phase was extracted with CH_2Cl_2 (3 × 100 mL). The combined organic phase was washed with 10% citric acid, 5% $NaHCO_3$, and brine, dried over anhydrous Na_2SO_4, filtered, and evaporated to provide crude product pinanediol ester, which was directly used in the next reaction.

To the solution of the prepared pinanediol ester (0.59 g, 1.00 mmol) and 2-methylpropylboronic acid (0.51 g, 5.00 mmol) dissolved in methanol (20 mL) and hexane (20 mL) was added 1 N HCl (2.5 mL). The reaction was stirred at room temperature for 18 h. The methanolic phase was washed with hexane

(3 × 15 mL), and the hexane layer was extracted with methanol (3 × 20 mL). The combined methanolic layers were evaporated in vacuo, and the residue was dissolved in CH_2Cl_2 (40 mL). The solution was washed with 5% $NaHCO_3$ (20 mL), and the organic layer was dried over anhydrous Na_2SO_4, evaporated, and purified with chromatography (CH_3OH:CH_2Cl_2 = 1:15 and then 1:3) to obtain 210 mg (46.8% yield) of a white foam solid **78**. ^{1}H NMR (CD_3OD, 500 MHz): δ 0.85−0.90 (−CH_3, m, 6H), 1.18−1.27 (−CH_2, m, 2H), 1.51−1.56 (−CH, m, 1H), 1.68−1.72 (−CH_2, m, 1H), 1.93−2.05 (−CH_2, m, 3H), 2.57−2.60 (−CH, m, 1H), 2.58−2.76 (−CH_2, m, 2H), 2.95−3.01 (−CH_2, m, 2H), 3.73−3.79 (−CH, m, 1H), 5.41−5.46 (−CH, m, 1H), 6.89−6.92 (-Ph, m, 1H), 6.98−7.00 (−Ph, m, 1H), 7.07−7.14 (−Ph, m, 3H), 7.16−7.18 (−Ph, m, 1H), 7.21−7.23 (−Ph, m, 1H), 7.34−7.40 (−Ph, m, 1H). ^{13}C NMR (CD_3OD, 125 MHz): δ 22.1, 23.8, 26.9, 28. 8, 30.2, 37.4, 41.0, 45.5, 47.9, 49.8, 51.0, 114.7, 115.7, 123.6, 127.0, 127.9, 129.9, 130.5, 131.7, 135.3, 138.9, 144.5, 165.4, 176.7, 177.6. MS (ESI) *m*/*z* (%) 477.2 (62) $[M + Na]^+$, 481.2 (100) $[M + 27]^-$. HRMS $[M + Na]^+$ calcd, 477.2336; found, 477.2327.

(*R*)-1-[3-(2-Naphthamido)-3-(3-fluorophenyl)propanamido]-3-methylbutyl Boronic Acid (79). A similar procedure was used as described with **78** with the corresponding starting materials. ^{1}H NMR (CD_3OD, 500 MHz): δ 0.83−0.88 (−CH_3, m, 6H), 1.20−1.25 (−CH_2, m, 1H), 1.26−1.30 (−CH_2, m, 1H), 1.50−1.58 (−CH, m, 1H), 2.63−2.66 (−CH, m, 1H), 3.12−3.15 (−CH_2, m, 1H), 3.18−3.21 (−CH_2, m, 1H), 5.68−5.72 (−CH, m, 1H), 7.02−7.06 (−Ph, m, 1H), 7.26−7.29 (−Ph, m, 1H), 7.31−7.34 (−Ph, m, 1H), 7.38−7.41 (−Ph, m, 1H), 7.54−7.61 (−Ph, m, 2H), 7.88−7.97 (−Ph, m, 3H), 7.98−8.02 (−Ph, m, 1H), 8.41−8.42 (−Ph, m, 1H). ^{13}C NMR (CD_3OD, 125 MHz): δ 22.0, 23.8, 27.0, 37.5, 41.0, 45.3, 51.8, 114.7, 115.8, 123.8, 125.0, 127.9, 128.5, 128.8, 129.0, 129.4, 130.0, 131.7, 132.5, 134.0, 136.4, 144.8, 163.8, 169.7, 177.0. MS (ESI) *m*/*z* (%) 473.1 (62) $[M + Na]^+$, 477.2 (100) $[M + 27]^-$. HRMS $[M + Na]^+$ calcd, 473.2023; found, 473.2030.

(*R*)-1-[3-(3-Fluorophenyl)-3-(5,6,7,8-tetrahydronaphthalene-4-carboxamid)propanamido]-3-methyl Butyl Boronic Acid (80). A similar procedure was used as described with **78** with the corresponding starting materials. ^{1}H NMR (CD_3OD, 500 MHz): δ 0.87−0.90 (−CH_3, m, 6H), 1.21−1.24 (−CH_2, m, 1H), 1.27−1.31 (−CH_2, m, 1H), 1.53−1.59 (−CH, m, 1H), 1.73−1.78 (−CH_2, m, 4H), 2.62−2.65 (−CH, m, 1H), 2.70−2.71 (−CH_2, m, 2H), 2.74−2.79 (−CH_2, m, 2H), 2.98−3.05 (−CH_2, m, 2H), 5.55−5.60 (−CH, m, 1H), 7.02−7.06 (−Ph, m, 1H), 7.11−7.15 (−Ph, m, 3H), 7.19−7.21 (−Ph, m, 1H), 7.26−7.27 (−Ph, m, 1H), 7.38−7.42 (−Ph, m, 1H). ^{13}C NMR (CD_3OD, 125 MHz): δ 22.1, 23.8, 24.0, 26.9, 27.6, 30. 7, 37.6, 41.0, 45.2, 49.8, 51.5, 114.8, 115.8, 123.8, 125.3, 126.4, 131.9, 135.5, 137.7, 139.2, 144.7, 165.4, 172.8, 176.7. MS (ESI) *m*/*z* (%) 477.2 (62) $[M + Na]^+$, 467.2 (100) $[M + 13]^-$. HRMS $[M + Na]^+$ calcd, 477.2336; found, 477.2329.

Proteasome Inhibition Assays. A 20S proteasome activity assay kit was purchased from Chemicon (Chemicon, United States). Other reagents and solvents were purchased from commercial sources. In brief, substrates and compounds were previously dissolved in DMSO, with the final solvent concentration kept constant at 3% (v/v). The reaction buffers were (pH 7.5) 20 mM Tris, 1 mM DTT, 10% glycerol, and 0.02% (w/v) DS for CT-L activities. The proteasome activity was determined by monitoring the hydrolysis of the fluorogenic substrate, Suc-Leu-Leu-Val-Tyr-AMC (λ_{exc} = 360 and λ_{exc} = 465 nm for AMC substrates), reacting for 1 h at 37 °C in the presence of untreated (control) or proteasome that had been incubated with a different concentration of test compounds. Fluorescence was measured using an Infinite M200 microplate reader (Tecan, Austria).

Cell Culture and Cytotoxicity Assays. BXPC-3 (human pancreatic cancer cell line), PC-3 (human prostate cancer line), HL-60 (promyelocytic leukemia cell line), and RPMI 8226 (multi myeloma cell line) human cell lines were obtained from the American Type Culture Collection (Manassas, VA). SW-480 (human colon carcinoma cell line), A549 (human nonsmall cell lung cancer cell line), SKOV-3 (human ovarian carcinoma), and HepG2 (human hepatocellular liver carcinoma cell line) cell lines were obtained from China Pharmaceutical University. HL-60 cells were cultured in IMDM supplemented with 20% fetal bovine serum at 37 °C in 5% CO_2. RPMI 8226 cells were cultured in RPMI 1640 supplemented with 10% fetal bovine serum at 37 °C in 5% CO_2. BXPC-3, HepG2, and SW-480 cells were grown in RPMI 1640 supplemented with 10% fetal bovine serum at 37 °C in 5% CO_2. PC-3 and A549 cells were cultured in F12-k supplemented with 10% fetal bovine serum at 37 °C in 5% CO_2. SKOV-3 cells were cultured in McCoy's 5A supplemented with 10% fetal bovine serum at 37 °C in 5% CO_2.

A standard MTT assay was used to measure cell growth. In brief, a suspension of 3000 cells/150 μL of medium was added to each well of 96-well plates and allowed to grow. Twenty-four hours later, drugs prepared in medium at 10 different concentrations were added to the corresponding plates at a volume of 50 μL per well, and the plates were incubated for 72 h with drugs. Then, 20 μL of a solution of 5 mg/mL MTT was added to each well and incubated for another 4 h at 37 °C. Plates were then centrifuged at 1000 rpm at 4 °C for 5 min, and the medium was carefully discarded. The formazan crystals were dissolved in 100 μL of DMSO, and absorbance was read on an Infinite M200 (Tecan, Austria) microplate reader at 540 nm. The result was expressed as the mean IC_{50} value, which was the average from at least three independent determinations.

Pharmacokinetic Analyses in Rodents. Solutions of **78**, **79**, **80**, and bortezomib were prepared in 1% ethanol, 1% Tween80, and 98% buffered saline with the final concentration of both compounds 0.5 mg/mL for iv and ig administration. Heparinized blood samples collected for PK analyses (n = 4) were centrifuged at 4000 rpm for 5 min at 4 °C. Plasma samples were analyzed after protein precipitation with acetonitrile acidified with 1% formic acid. LC/MS/MS analysis of **78**, **79**, **80**, and bortezomib was performed under optimized conditions to obtain the best sensitivity and selectivity of the analyte in selected reaction monitoring mode (SRM). Selected product ions of **78**, **79**, and **80** were monitored for the quantification of the compound using bortezomib as an internal standard. Plasma concentration−time data were analyzed by a noncompartmental approach using the software WinNonlin Enterprise version 5.2 (Pharsight Co., Mountain View, CA).

Acknowledgment. We thank Dr. Xin Cao, State Key Laboratory of Bioorganic and Natural Products Chemistry Shanghai Institute of Organic Chemsitry, Chinese Academy of Sciences, for his manuscript reading.

Note Added after ASAP Publication. This paper published on the web on November 15, 2010 with errors in the author affiliations. The correct version was published on November 18, 2010.

Supporting Information Available: General and experimental procedures and characterization data for **4A1**−**4A48**, **6**, **9**, **10a**−**10j**, **12a**−**12j**, **14**−**77**, and **81**−**85**. This material is available free of charge via the Internet at http://pubs.acs.org.

References

(1) Glickman, M. H.; Ciechanover, A. The ubiquitin-proteasome proteolytic pathway: Destruction for the sake of construction. *Physiol. Rev.* **2002**, *82*, 373–428.
(2) Hershko, A.; Ciechanover, A. The ubiquitin system. *Annu. Rev. Biochem.* **1998**, *67*, 425–479.
(3) Pickart, C. M. Mechanisms underlying ubiquitination. *Annu. Rev. Biochem.* **2001**, *70*, 503–533.
(4) Borissenko, L.; Groll, M. 20S proteasome and its inhibitors: crystallographic knowledge for drug development. *Chem. Rev.* **2007**, *107*, 687–717.
(5) Kisselev, A. F.; Akopian, T. N.; Castillo, V.; Goldberg, A. L. Proteasome active sites allosterically regulate each other, suggesting a cyclical bite-chew mechanism for protein breakdown. *Mol. Cell* **1999**, *4*, 395–402.
(6) Adams, J. The development of proteasome inhibitors as anticancer drugs. *Cancer Cell* **2004**, *5*, 417–421.

(7) Dispenzieri, A. Bortezomib for myeloma—Much ado about something. *N. Engl. J. Med.* **2005**, *352*, 2546–2548.
(8) Cavo, M. Proteasome inhibitor bortezomib for the treatment of multiple myeloma. *Leukemia* **2006**, *20*, 1341–1352.
(9) Richardson, P. G.; Sonneveld, P.; Schuster, M. W.; Irwin, D.; Stadtmauer, E. A.; Facon, T.; Harousseau, J. L.; Yehuda, B. D.; Lonial, S.; Goldschmidt, M. B.; Cavenagh, J.; Dalton, W. S.; Boral, A. L.; Esseltine, D. L.; Porter, J. B.; Schenkein, D.; Anderson, K. C. Bortezomib or high-dose dexamethasone for relapsed multiple myeloma. *N. Engl. J. Med.* **2005**, *352*, 2487–2498.
(10) O'Connor, O. A. Marked clinical activity of the proteasome inhibitor bortezomib in patients with follicular and mantle-cell lymphoma. *Clin. Lymphoma Myeloma* **2005**, *6*, 191–199.
(11) Fisher, R. I.; Bernstein, S. H.; Kahl, B. S.; Djulbegovic, B.; Robertson, M. J.; de Vos, S.; Epner, E.; Krishnan, A.; Leonard, J. P.; Lonial, S.; Stadtmauer, E. A.; O'Connor, O. A.; Shi, H.; Boral, A. L.; Goy, A. Multicenter phase II study of bortezomib in patients with relapsed or refractory mantle cell lymphoma. *J. Clin. Oncol.* **2006**, *24*, 4867–4874.
(12) Richardson, P. G.; Barlogie, B.; Berenson, J.; Singhal, S.; Jagannath, S.; Irwin, D.; Rajkumar, S. V.; Srkalovic, G.; Alsina, M.; Alexanian, R.; Siegel, D.; Orlowski, R. Z.; Kuter, D.; Limentani, S. A.; Lee, S.; Hideshima, T.; Esseltine, D. L.; Kauffman, M.; Adams, J.; Schenkein, D. P.; Anderson, K. C. A phase 2 study of bortezomib in relapsed, refractory myeloma. *N. Engl. J. Med.* **2003**, *348*, 2609–2617.
(13) Ludwig, H.; Khayat, D.; Giaccone, G.; Facon, T. Proteasome inhibition and its clinical prospects in the treatment of hematologic and solid malignancies. *Cancer* **2005**, *104*, 1794–1807.
(14) Zhu, Y. Q.; Zhao, X.; Zhu, X. R; Wu, G.; Li, Y. J.; Ma, Y. H.; Yuan, Y. X.; Yang, J.; Hu, Y.; Ai, L.; Gao, Q. Z. Design, synthesis, biological evaluation, and structure-activity relationship (SAR) discussion of dipeptidyl boronate proteasome inhibitors, part I: Comprehensive understanding of the SAR of α-amino acid boronates. *J. Med. Chem.* **2009**, *52*, 4192–4199.
(15) Zhu, Y. Q.; Yao, S. Y; Xu, B.; Ge, Z. M.; Cui, J. R.; Chen, T. M.; Li, R. T. Design, synthesis and biological evaluation of tripeptide boronic acid proteasome inhibitors. *Bioorg. Med. Chem.* **2009**, *17*, 6851–6861.
(16) Cardillo, G.; Tomasini, C. Asymmetric synthesis of β-amino acids and α-substituted β-amino acids. *Chem. Soc. Rev.* **1996**, *25*, 117–128.
(17) Nicolaou, K. C.; Guy, R. K. The conquest of Taxol. *Angew. Chem., Int. Ed. Engl.* **1995**, *34*, 2079–2090.
(18) Shinagawa, S.; Kanamaru, T.; Harada, S.; Asai, M.; Okazaki, H. Chemistry of emeriamine and its analogs and their inhibitory activity in long-chain fatty acid oxidation. *J. Med. Chem.* **1987**, *30*, 1458–1463.
(19) Ford, P. W.; Gustafson, K. R.; McKee, T. C.; Shigematsu, N.; Maurizi, L. K.; Pannell, L. K.; Williams, D. E.; de Silva, E. D.; Lassota, P.; Allen, T. M.; Van Soest, R.; Andersen, R. J.; Boyd, M. R.; Papuamides, A-D HIV-inhibitory and cytotoxic depsipeptides from the sponge theonella mirabilis and theonella swinhoei collected in Papua new Guinea. *J. Am. Chem. Soc.* **1999**, *121*, 5899–5909.
(20) Wani, M. C.; Taylor, H. L.; Wall, M. E.; Coggon, P.; McPhail, A. T. Plant Antitumor Agents. VI. The isolation and structure of Taxol, a novel antileukemic and antitumor agent from Taxus brevifolia. *J. Am. Chem. Soc.* **1971**, *93*, 2325–2327.
(21) Roncari, G.; Kurylo-Borowska, Z.; Craig, L. C. On the chemical nature of the antibiotic edeine. *Biochemistry* **1966**, *5*, 2153–2159.
(22) Gould, S. J.; Thiruvengadam, T. K. Studies of nitrogen metabolism using C-13 NMR spectroscopy. 3. Synthesis of DL-[3−13C, 2−15N]lysine and its incorporation into streptothricin F1. *J. Am. Chem. Soc.* **1981**, *103*, 6752–6754.
(23) Hinterman, T.; Seebach, D. The biological stability of β-peptides: No interactions between α- and β-peptidic structures? *Chimia* **1997**, *51*, 244–247.
(24) Zhu, Y. Q.; Zhu, X. R.; Wu, G.; Ma, Y. H.; Li, Y. J.; Zhao, X.; Yuan, Y. X.; Yang, J.; Yu, S.; Shao, F.; Li, R. T.; Ke, Y. R.; Lu, A. J.; Liu, Z. M.; Zhang, L. R. Synthesis, in vitro and in vivo biological evaluation, docking studies and structure-activity relationship (SAR) discussion of dipeptidyl boronic acid proteasome inhibitors composed of β-amino acids. *J. Med. Chem.* **2010**, *53*, 1990–1999.
(25) Klausner, Y. S.; Bodansky, M. Coupling reagents in peptide synthesis. *Synthesis* **1972**, 453–463.
(26) Pallombella, V. J.; Conner, E. M.; Fuseler, J. W.; Destree, A.; Davis, J. M.; Laroux, F. S.; Wolf, R. E.; Huang, J.; Brand, S.; Elliott, P. J.; Lazarus, D.; Parent, L.; Stein, R.; Adams, J.; Grisham, M. B. Role of the proteasome and NF-kappa B in streptoccal cell wall-induced polyarthritis. *Proc. Natl. Acad. Sci. U.S.A.* **1998**, *95*, 15671–15676.
(27) Teicher, B. A.; Ara, G.; Herbst, R.; Palombella, V. J.; Adams, J. The proteasome inhibitor PS-341 in cancer therapy. *Clin. Cancer Res.* **1999**, *5*, 2638–2645.